Superior carbon nanotube stability by molecular filling:a single-chirality study at extreme pressures.

Colin Bousige, Aude Stolz, Silvio D Silva-Santos, Jingming Shi, Wenwen Cui, Miguel A.L. Marques, Chunyang Nie, Emmanuel Flahaut, Marc Monthioux, Alfonso San-Miguel

Superior carbon nanotube stability by molecular filling: a single-chirality study at extreme pressures.

Colin Bousige[a,*], Aude Stolz[b], Silvio D. Silva-Santos[b], Jingming Shi[c], Wenwen Cui[c], Chunyang Nie[d,e], Miguel A.L. Marques[f], Emmanuel Flahaut[d], Marc Monthioux[e], Alfonso San-Miguel[b,*]

[a] *Laboratoire des Multimatériaux et Interfaces, UMR CNRS 5615, Univ. Lyon, Université Claude Bernard Lyon 1, F-69622 Villeurbanne, France*
[b] *Institut Lumière Matière, UMR CNRS 5306, Univ Lyon, Université Claude Bernard Lyon 1, F-69622 Villeurbanne, France*
[c] *School of Physics and Electronic Engineering, Jiangsu Normal University, Xuzhou 221116, China*
[d] *CIRIMAT, Université de Toulouse, CNRS, INPT, UPS, UMR CNRS-UPS-INP N.5085, Université de Toulouse 3 Paul Sabatier, Bât. CIRIMAT, 118, route de Narbonne, 31062 Toulouse cedex 9, France*
[e] *Centre d'Elaboration des Matériaux et d'Etudes Structurales (CEMES), UPR-8011 CNRS, Université de Toulouse, 29 rue Jeanne Marvig, 31055 Toulouse, France*
[f] *Institut für Physik, Martin-Luther-Universität Halle-Wittenberg, 06120 Halle (Saale), Germany*

Abstract

Carbon nanotubes have extraordinary mechanical properties, but modifications of their structure tend to weaken them. Here, we have studied by experiments and modelling the one-dimensional filling of single chirality (6,5) carbon nanotubes with iodine and water. We show that iodine-filling can enhance the pressure of radial collapse of these nanotubes by a factor 2 compared to the empty (6,5) tubes. For water filling, this enhancement factor reduces to 1.4. Our single-chirality study allows correlating the different Raman signatures of the radial collapsing process, which was not possible in samples with mixed chiralities. A clear spectroscopic signature of the collapse pressure can thus be given: it is the pressure at which the G-band frequency evolution with pressure softens while the radial breathing mode intensity vanishes. These new criteria for the detection of radial collapse allow correcting some existing discrepancies in the literature. Finally, we discuss the impact of molecular filling on the radial mechanical stability as a function of the tube diameter. It results that molecular filling allows for a superior stability effect than filling with tubes (*i.e.* multi-wall carbon nanotubes). The stability enhancement tends to grow with the tube diameter and depends strongly on the nature of the filling molecules.

Keywords: carbon nanotubes, single chirality, high pressure, radial collapse, nanotube filling, enhanced mechanical stability

*Corresponding authors
Email addresses: colin.bousige@univ-lyon1.fr (Colin Bousige), alfonso.san-miguel@univ-lyon1.fr (Alfonso San-Miguel)

1. Introduction

Carbon nanotube geometry is an important parameter when considering their mechanical properties. In fact, whereas the extraordinary mechanical properties of single-wall carbon nanotubes (SWCNT) are essentially diameter-independent and linked to the sp^2 in-plane graphene mechanical properties [1], it is quite different for the radial mechanical properties which are determined by the nanotube diameter [2–5]. SWCNT can be uniquely defined by their chiral indices (n, m), a vector defined in a graphene plane determining how to roll it to obtain a nanotube. The chirality determines the electronic (metallic or semiconducting) and peculiar optical properties of SWCNT [6]. From a geometrical point of view, different chiral indices can give rise to very similar values of nanotube diameter. The mechanical properties of SWCNT are considered to be diameter and not chirality dependent with perhaps some exceptions for low chiral indices [7].

More particularly, the phase diagram of empty SWCNT shows that they are mechanically stable in a limited diameter domain comprised between 0.44 nm and ∼5 nm [5, 8]. Outside of this domain, either free-standing tubes do not exist (for lower diameters) or they are found in a radially collapsed geometry (for larger diameters). Applying pressure leads to the radial collapse of SWCNT [2–5] with a pressure of radial collapse which can be well reproduced by continuum mechanics in a diameter domain comprised between ~ 1 nm and ~ 2.5 nm [5].

Carbon nanotube molecular filling offers a route to simultaneously modify the physico-chemical properties of SWCNT [9, 10] and increase their mechanical stability while protecting the encapsulated 1-D molecular structure [11, 12]. Endohedral intercalation thus offers a route for physico-chemical modifications, while avoiding bonding to other chemical species or creating defects, which both are mechanisms that introduce mechanical unstability [13]. Nanotube filling is not expected to affect the axial stiffness and strength, whereas the radial mechanical properties may be significantly improved [7, 12, 14]. All these considerations are particularly important for applications in nanocomposite materials which may be submitted to different mechanical efforts [15–17], or in pressure- or strain-driven devices based on carbon nanotubes [18, 19].

There have been many studies probing the mechanical, electronic, vibrational or structural properties of single wall carbon nanotubes at high pressure, using X-ray or neutron diffraction [20, 21], photoluminescence [7, 22], optical absorption spectroscopy [23, 24], electronic transport measurements [25] but the studied samples have been mostly composed of mixtures of nanotubes with different chiralities or, in the very few cases in which a unique carbon nanotube has been studied at high pressure, its chirality was not identified [18]. There is thus a lack of studies of *single chirality* samples at high pressure, studies that would allow correlating the pressure evolution of properties with a given chirality or diameter, as well as the effect of molecular filling on these properties. This is particularly important when comparing experimental results with results obtained from atomistic modelling which are performed for a single type of nanotube with, therefore, a single well-defined chirality.

The above considerations also apply to Raman spectroscopy. In fact, Raman spectroscopy is a very sensitive characterization tool widely used for investigating the mechanical and electronic properties of CNT under extreme conditions – mainly under compression – allowing following *in situ* structural transformations [7, 26–36]. The Radial Breathing Mode (RBM) offers an accurate measurement of the structural tunability, since its frequency is inversely proportional to the SWCNT diameter and its intensity is strongly dependent on the optical transition energies. The RBM therefore constitutes an accurate probe of the radial deformation and the nanotube radial collapsing process. Furthermore, because it is related to the E_{2g} modes, the G-band constitutes an accurate probe of the strain and doping in sp^2 systems such as carbon nanotubes [37] or graphene [38, 39]. In SWCNT, the G-band is usually split into its G^+ and G^- components, related to the E_{2g} modes propagating either along the tube axis or its circumference, respectively. However, while the RBM position and intensity is directly dependent on the nanotube chirality, the G^+ and G^- components only show a poor dependence on the chirality and diameter – with an increased dependence on the diameter for the G^- mode, as small diameters induce large out-of-plane constraints on the sp^2 bonds. As a consequence, in a sample of SWCNT with mixed chiralities, while each RBM peak corresponds to a given individual chirality, the G-band always arises from the mixture of all chiralities. A study performed on a single-chirality sample would thus provide the intrinsic G-band response of a single nanotube chirality to an external constraint such as pressure, opening the path for an accurate direct confrontation between experiments and atomistic models.

In this paper, we investigate the mechanical stability of SWCNT samples with a high proportion of (6,5) chirality, either individualized or in bundles, in three cases: empty, water-filled, or iodine-filled. We investigate, through experiments and atomistic modelling, the effect of molecular filling on the radial stability of SWCNT by studying samples with mostly a single chirality. From the experimental point of view, Raman spectroscopy allows correlating pressure-induced changes in the tube geometry thanks to signature evolutions both in the RBM and in the G-band Raman signal *for a single chirality*. This correlation has been in fact up to now not possible due to the study of mixed chirality samples.

2. Experimental and computational methods

Chirality-selected (6,5) SWCNT were obtained using the Aqueous Two-Phase Separation (ATP) method [40, 41] from a CoMoCAT SWCNT powder (Sigma-Aldrich, SG65i) – initially containing a large proportion ($\gtrsim 45\,\%$) of (6,5) SWCNT. First, a Stock 1 mg/mL nanotube dispersion was obtained by sonication in 1 % aqueous sodium deoxycholate (DOC) solution. Then, two surfactant-polymer solutions (S1 and S2) were prepared using polyethylene glycol (PEG), dextran, DOC, sodium dodecyl sulfate (SDS) and sodium cholate (SC) – the full details are gathered in Tab. S1. The stock nanotube solution added with S1 was then centrifuged at 9500 rcf. The bottom solution was collected, mixed with

S2, and centrifuged again. The top phase, now containing a majority of (6,5) SWCNT (Fig. 1(a)), was then collected and submitted to a cycle of washing in water and ethanol, filtration, and annealing at 600 °C in argon to remove the polymers surrounding the nanotube bundles. To allow the nanotubes to be filled, they then need to be opened. For that purpose, part of the nanotubes were heated up to the temperature of 550 °C in air with a ramp of 10 °C/min and then collected as soon as the target temperature was achieved. Aiming for a 10 % mass loss, this annealing allows to selectively open the nanotubes around the reactive sites located at the tips and the defects [42, 43]. Further details on this sample preparation are reported in the SI, as well as a photo-luminescence excitation map of the Stock and final solutions (Fig. S1).

To fill the (6,5) SWCNT with iodine, a mixture of molar ratio 1:1.3 SWCNT buckypaper:iodine powder was ground in a mortar. The mixture was then transferred into a quartz ampule (6 mm diameter) using a glass funnel. As iodine is sensitive to air, the above steps were performed in a tent under N_2 atmosphere. Subsequently, the ampule was evacuated down to a reduced pressure of 20 Pa and kept subjected to this dynamic vacuum for 2 h. Finally, the ampule was sealed by local melting with a flame and placed into a furnace to be heated up to 140 °C for 24 h. The iodine-filled (6,5) SWCNT (I@SWCNT65) were then washed in absolute ethanol until the liquid was colorless [44]. From Raman characterization (Fig. 1(b)), the filling rate appeared to be close to 80 % (assuming that the empty and filled nanotubes display the same RBM Raman cross-section, which might not be the case). This is a remarkable filling rate which was not able to be achieved for nanotube samples made of random diameters. The filling efficiency is of the same range as that of C_{60} molecules when filling SWCNT material containing a majority of (10,10) tubes. This supports the statement that the main limitation to high filling rate of SWCNT with molecules is the presence of a fraction of CNT whose diameters are not energetically optimized for hosting the molecules involved – essentially, the CNT inner cavity needs to be of similar diameter than the wanted molecules to favor their adsorption. This is out of the scope of this paper, but considering the high doping power of iodine with respect to SWCNT (or DWCNT), a I@SWCNT65-based material would be worth studying regarding its transport properties. Figure 1(c) shows a high angle annular dark field TEM image of I@SWCNT65: many single-atom iodine chains (bright contrast) can be seen, which confirms that iodine fills the tube cavities. Raman spectroscopy of the nanotubes before and after the filling procedure (Fig. 1(b)) shows that the (6,5)-associated RBM mode is highly blue-shifted by the insertion of iodine, from 295 cm^{-1} to 323 cm^{-1}. In spite of the filling procedure, the empty-tube RBM signal is still clearly visible at 295 cm^{-1}, which allows independently following the evolution of both empty and filled tubes under pressure. Unfortunately, the complexity of the resonance Raman process [45, 46], with the present knowledge, does not allow for a precise quantification of the filling degree beyond the rough estimate of 80 % filling. From the Raman signal only, it is impossible to distinguish between the case where 80 % of the tubes are fully filled and 20 % are empty, the case where 100 % of

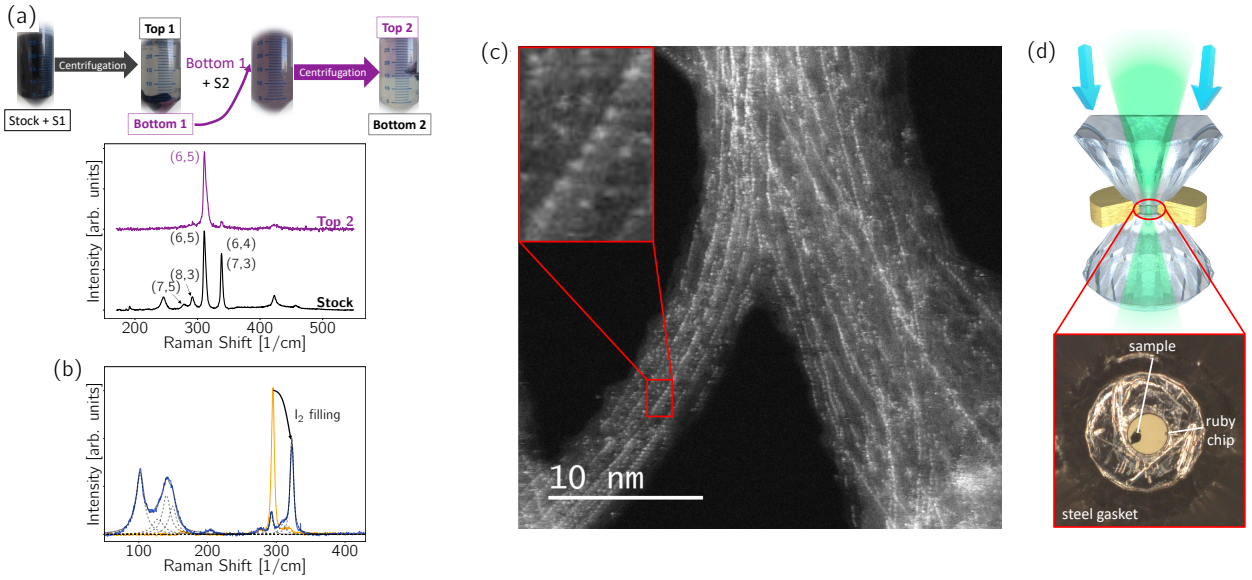

Figure 1: (a) Schematics of the ATP procedure for separating nanotubes per chirality. The final solution, Top 2, contains a large majority of (6,5) SWCNT as can be seen by the purple color of the solution, which is confirmed by Raman spectroscopy (568.2 nm excitation laser). – (b) Raman spectra of the (6,5) nanotubes before (orange) and after (blue) filling with I_2 (532 nm excitation laser). Dashed grey lines are Lorentzian fits of the I@SWCNT65 spectrum. The four peaks fitting the iodine features are centered at 102, 128, 140 and 149 cm^{-1} at ambient pressure. – (c) HAADF-TEM image of the iodine-filled (6,5) nanotubes. Single-atom chains of iodine can clearly be seen as lines of bright dots, as highlighted in the zoomed area. Another image is shown in Fig. S2. – (d) Upper image: schematics of the Diamond Anvil Cell apparatus principle showing the interior of the experimental cavity defined between the diamonds and the metallic gasket. Enlargement: optical image of the sample chamber taken through one of the diamonds showing a nanotube sample immersed in the liquid pressure transmitting medium and a ruby chip used for pressure calibration. On this picture, the sample chamber hole diameter is ~ 120 μm.

the tubes are filled at 80 %, and the case where a mixture of both previous scenarios occurs. The HRTEM images seem to show that when the tubes are filled, they are filled with a high degree (see Fig. S2 for a larger image). Although HRTEM images are very local and might not be a reflection of the entirety of the sample, this observation goes in the direction of the sample being a mixture of highly filled tubes and empty ones, i.e. the ones that were not opened or not accessible for iodine filling.. Fig. 1(b) also shows the additional iodine signal in I@SWCNT65 between $\sim$ 102 and $\sim$ 143 cm^{-1}.

A fraction of I@SWCNT65 powder was placed inside the diamond anvil cell (DAC) (Fig. 1(d)) using a tungsten tip together with a small ruby chip for pressure measurement using ruby fluorescence calibration [47]. A 4:1 methanol-ethanol mixture was used as pressure transmitting medium (PTM), as this alcohol mixture remains liquid (and thus perfectly hydrostatic) up to 10.5 GPa [48]. The pressure was exerted through a deformable membrane applying the driving force on the DAC piston [49], up to a maximum pressure of 51 GPa (Fig. 1(d)). At such high pressures, the nanotubes were mostly destroyed [50] and reversibility was thus not ob-

served (Fig. 2(a)).

The Raman spectra were recorded using a LabRAM HR Evolution micro-Raman spectrometer (Horiba Jobin-Yvon), with an excitation laser line of 2.33 eV (532 nm). The scattered light was collected in back-scattering geometry through the diamond anvil and using a ×50 long-working distance objective (Fig. 1(d)). The laser power was increased as much as possible while checking that the Raman signatures were not changing in position and shape, and power was kept below $\sim$ 3.2 mW (before going through the diamond anvil). The scattered light was dispersed by a 1800 grooves/mm grating, allowing for a spectral resolution of $\sim$ 1 cm^{-1}. The Raman spectra are then subtracted of a polynomial background and fitted using Lorentzian or Voigt functions (Voigt functions are only used for iodine peaks above 15 GPa).

The calculations of the collapse of the empty and filled with iodine and water CNT were carried out by using the density functional tight-binding (DFTB) method [51], as implemented in the DFTB+ package [52]. DFTB method has successfully been used simulate both empty [3, 4, 53] and filled CNT [11]. The parameters to describe the carbon-carbon interaction were taken from the matsci-0-3 set, [54] while we used halorg-0-1 [55] set for iodine-iodine and iodine-carbon, and mio-1-1 set [56] for oxygen-oxygen, hydrogen-hydrogen, carbon-oxygen, carbon-hydrogen and oxygen-hydrogen interactions. Computations were performed on a single (6,5) nanotube unit, the cell containing 364 carbon atoms (twice that number in the bundle case where two adjacent tubes were considered), and having an initial dimension of $10.8 \times 10.8 \times 40.64$ $Å^3$. Various filling conditions were considered: empty tubes, empty tubes in a bundle, tubes filled with 14 water molecules, and tubes filled with 6 or 7 I_2 molecules.

3. Results

Figure 2 displays the pressure evolution of the Raman spectra of I@SWCNT65. The first two bands at 102 and 143 cm^{-1} are attributed to the iodine polyanions I_3^- and I_5^- forming inside the tubes, respectively [14, 57–59]. We observe that the position of these two bands at ambient pressure in our tubes is significantly lower than the one observed in the case of iodine inside tubes of $\sim$1.4 nm diameter (109 and 174 cm^{-1}) [14]. We also note that in our case, only 4 contributions to these bands (or even 2 at higher pressures) are necessary to fit our spectra (Fig. 1(b)), whereas for larger and more dispersed diameter distributions, up to 7 peaks were necessary [14]. This can be explained by the fact that 1.4 nm diameter nanotubes allow for nonlinear polyiodine structures such as L and V-shaped I_5^- [14], while the $\sim$ 7.5 Å diameter of (6,5) SWCNT only allows for single-file structures. We thus expect the Raman spectrum of I@SWCNT65 to show different spectral contributions depending on nanotube diameter. Moreover, higher energy contributions are attributed to nonlinear polyiodine chains [14, 60], and their absence thus shifts the spectrum to lower frequencies – which matches our observations.

The pressure evolution of the position and width of the iodine components is presented in Fig. 2(b-d). As soon as the pressure increases, only three

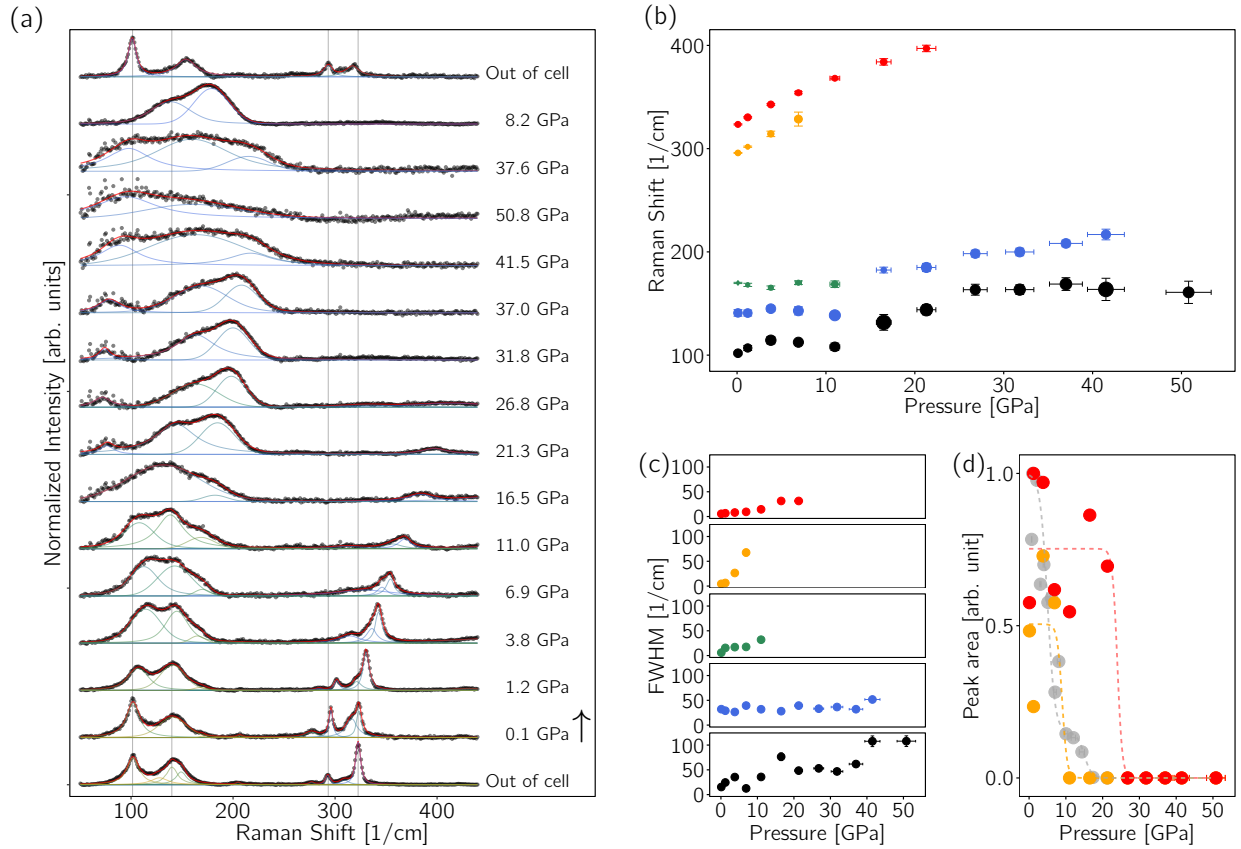

Figure 2: (a) Pressure evolution of the Raman spectra of I@SWCNT65, focused on the RBM and iodine modes. The lines correspond to Lorentzian/Voigt fits of the experimental data (points). For clarity, the spectra are normalized to the maximum intensity in this energy range, and then vertically shifted. The vertical lines are guides for the eye indicating the position of the prominent peaks of polyiodine and empty/filled (6,5) nanotubes at room pressure. – Pressure evolution of the Raman RBM and iodine peaks positions (b) and FWHM (c). Point size in (b) is proportional to normalized peak integrated intensity. The lower frequency RBM peaks ($\sim$ 296 cm^{-1} at room pressure) correspond to the empty tubes. – (d) Pressure evolution of the RBM peak area for I@SWCNT65 (red) and empty (6,5) nanotubes (orange) in alcohol PTM. The gray signs correspond to water-filled individualized (6,5) nanotubes in the Top 2 solution (Fig. 1(a)). This solution contains both empty and water-filled nanotubes, and the PTM is a mixture of water, polymers and surfactants. Full fits of the water-filled sample are available in Figs. S4 and S5. Dashed lines are guides to the eyes. In all panels, the vertical error bars are fitting standard errors, while the horizontal ones come from the standard 5 % incertitude on pressure determination [47] – the same applies to Fig. 3.

Lorentzian components are needed to fit the iodine peaks (four at room pressure) – and this goes down to two Voigt components for pressures above 15 GPa. In the [0,10] GPa range, the iodine components are little affected by the increase in pressure: the nanotube host screens the adsorbed iodine from the applied pressure. For pressures between 10 and 30 GPa however, a 60 cm^{-1} blueshift is observed. This coincides with an increasing facetization of the nanotubes together with progressive polymerization between adjacent tubes, as simulated by DFTB and shown in the snapshots dis-

played in Fig. S6. Moreover, for pressures above 30 GPa, no further evolution of the iodine peaks is observed, although they disappear at $\sim$ 50 GPa. The peaks are retrieved when decreasing the pressure, but the higher energy peak is now shifted to 154 cm^{-1} at room pressure (143 cm^{-1} before the pressure cycle).

The pressure evolution of the RBM peak position, width, and intensity is shown in Fig. 2(b-d). The disappearing of the RBM signal shows that the empty tubes (orange points) collapse around 9 GPa, while the iodine-filled ones (red points) collapse at a much higher pressure of $\sim$ 24 GPa – which corresponds to an enhanced mechanical resistance to pressure for filled nanotubes [14, 32]. The same effect of an increased collapse pressure is observed for water-filled individual (6,5) nanotubes (gray points in Fig. 2(d)), but with a collapse pressure of $\sim$ 15 GPa. Iodine filling thus seems to greatly enhance the mechanical properties of such small nanotubes compared to water filling.

These observations are confirmed by the evolution of the G-band with pressure shown in Fig. 3. The latter shows a linear blueshift with pressure for both water-filled and iodine-filled (6,5) SWCNT up to the critical pressures of $\sim$16 and $\sim$24 GPa, respectively. Above these critical pressures, the pressure evolution of the G-band position moves towards the pressure behavior of graphite [32, 34, 62], indicating that the nanotubes are fully collapsed. The full spectra are shown in Fig. S3. In Fig. 3, we can also observe the convergence of the G$^+$ and G$^-$ components towards the graphite behavior. This is not observed in mixed chirality tubes [7] and could constitute an additional signature of the pressure-induced collapse which needs the study of single chirality tubes to be put into evidence. We only show the two components of the G-band for the iodine-filled tubes in which we could estimate a dominant proportion of filled tubes.

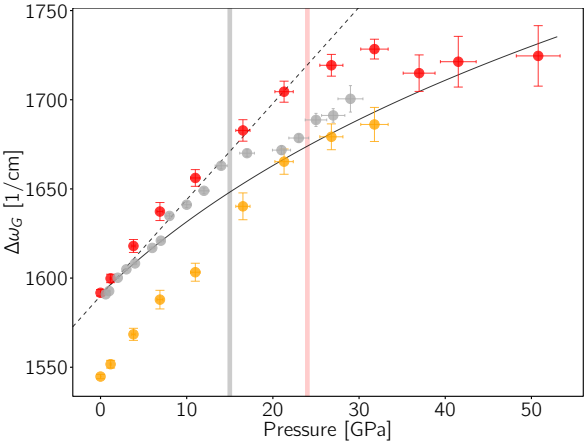

Figure 3: Pressure evolution of the Raman G-band shift. I@SWCNT65 data are shown in red for the G$^+$ component and orange for the G$^-$ one, while data for the individualized water-filled tubes from the Top 2 sample are shown in gray (G$^+$ only for clarity). The full line corresponds to the graphite equation of state [61], while the dashed line is a guide for the eye corresponding to the linear fit of low-pressure data. The vertical lines mark the onset of collapsing pressures of 15 and 24 GPa determined from the observation of the RBM peaks. Above 26.8 GPa, the G$^-$ component become indiscernible in I@SWCNT65.

Interestingly, a wide range of collapsing pressures are predicted with our DFTB computations for (6,5) SWCNT in various conditions. For empty nanotubes, Fig. 4 shows that the interaction of the tubes with their neighbors has a tremendous effect on the collapsing pressure, going from $\sim$ 24.1 GPa for single tubes down to $\sim$ 15.7 GPa for bundles of two nanotubes (see Fig. S6 for further details on the intermediate structures). Note that given the large number of atoms in a (6,5) SWCNT unit cell,

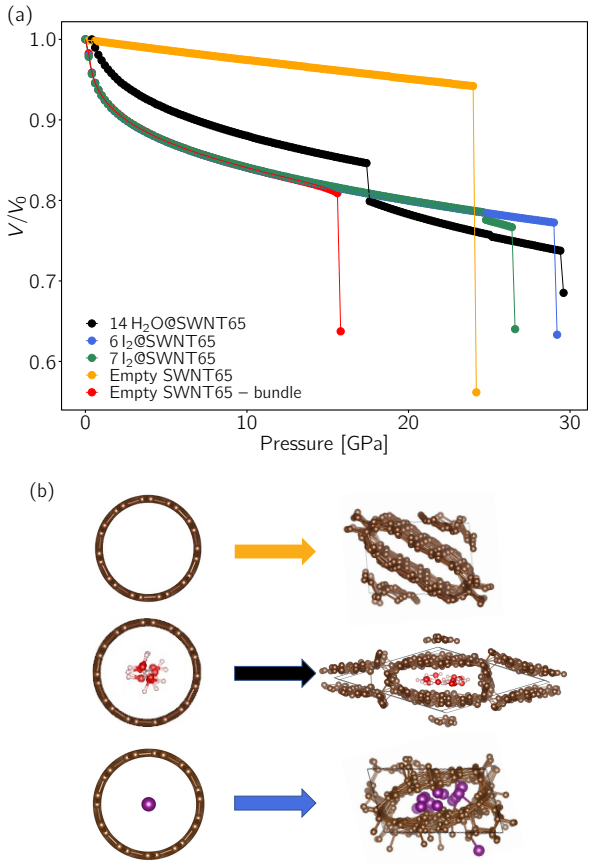

Figure 4: (a) DFTB-computed relative variation of volume as a function of pressure for (6,5) SWCNT filled with different molecules (H_2O and I_2). Except when specified (bundle), a single tube was considered in the simulation box. In the bundle case, the simulation box contains two tubes. – (b) Snapshots of the cross-section of the main simulated structures, at 0 pressure and at the maximum pressure reached. More details and intermediate structures are shown in Fig. S6.

only one or two tubes were considered in the DFTB simulations to keep the computation feasible. Further increasing the number of nanotubes in a bundle might lead to the decreasing of the predicted collapsing pressure, hence approaching experimental observations.

4. Discussion

First of all, we underline that our Raman study on single chirality (6,5) tubes allows to unequivocally correlate the different Raman spectroscopic signatures of the radial collapse. The RBM disappearance is observed in Fig. 2.(d) at 15-16 and 22-24 GPa for water-filled and iodine-filled (6,5) tubes respectively. These are exactly the same pressure values for which the G-band position deviates from linearity with an associated softening for these same (6,5) filled tubes (Fig. 3). This is a remarkable result as in many previous works the collapse pressure was identified as related to a change of sign in the G-band pressure derivative of the wavelength [10, 32]. We do also observe this effect, but at a pressure 25 % higher than the collapse one. Collapse pressures have therefore been overestimated in many works, which can now be corrected using the collapse pressure criteria for the G-band here obtained.

Table 1 summarizes the collapse pressures obtained by the different experimental and calculation methods used in our work. The DFTB values correspond to the first collapse observation with the largest supercell as it will be discussed below. We have also included results from the modified Lévy-Carrier (mLC) formula proposed in Ref. [4] as $P_C d^3 = 24\alpha D(1-\beta^2/d^2)$, with D the graphene bending stiffness, β the lowest diameter for a free standing tube, and α a coefficient having a value of 1.0 for the collapsing onset and 1.5 for the collapsing end, as proposed in Ref. [63].

Overall, there is an excellent consistency and agreement between experiments, DFTB modelling

Table 1: Collapse pressures P_c (in GPa), obtained from the RBM and G-band evolution of our Raman experiments and DFTB modelling (for the largest simulation cell). Included are the prediction of the collapsing onset and end of collapsing from the modified Lévy-Carrier model [4] and this same model including bundles. The two slash-separated values correspond to observations or predictions for the onset and end of the collapsing process, respectively.

	(6,5)	I_2@(6,5)	H_2O@(6,5)
RBM	9	22	15
G-band	-	24/35	16
DFTB	15.7	29	17.5
mLC	10.2/15.7	-	-
mLC bundles	9.6/14.4	-	-

and predictions from the mLC model. For filled nanotubes, defining their collapse pressure from DFTB calculations is not as straightforward as for the empty ones, as can be seen from the various snapshots of Fig. S6. Taking water-filled nanotubes as an example, a sequence of two volume drops at 17.5 GPa and 29.5 GPa takes place, rending difficult the definition of a unique collapse pressure. Taking the first volume drop as criterion for the collapse pressure, the simulations reproduce the trend of having a much larger collapse pressure for iodine-filled tubes ($\sim$ 29 GPa) than for water-filled ones ($\sim$ 17 GPa). This is then the criterion retained in Table 1. These pressures are however 20 % and 13 % larger, respectively, than the ones observed experimentally – but this can be explained by the bundle effect observed for empty nanotubes (Fig. 4), or even due to non-hydrostatic effects as in bundle-bundle contacts which are not considered in our atomistic modelling.

Both experiments and calculations point to a very weak effect of water-filling on the mechanical stability of the (6,5) tubes with pressure. On the contrary, iodine filling leads to a considerable extension of the stability domain of the order of 100 % with respect to the empty (6,5) tube.

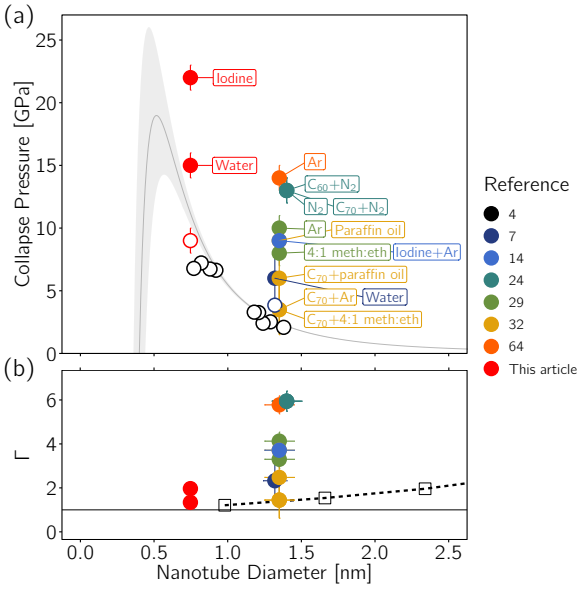

Figure 5: (a) Onset of the collapse pressure versus nanotube diameter: comparison between the modified Lévy-Carrier model [4] and some experimental values from the present work and Refs. [4, 7, 14, 24, 29, 32, 64] after applying our spectroscopic criterion for collapse pressure determination. The shaded area corresponds to the error bar around the parameter $\beta = 0.44 \pm 0.04$ in the modified Lévy-Carrier model [4]. The open signs correspond to empty tubes, while the solid signs are for filled tubes with the indicated fillers. – (b) Pressure evolution of $\Gamma = P_c^f / P_c^e$ for the same points as in panel (a). The reference P_c^e is taken as the value given by the modified Lévy-Carrier model [4]. The horizontal line marks the value $\Gamma = 1$. The dashed line and empty squares show the expected value of Γ for tubes filled with nanotubes [4], using as smallest inner-tube diameter a value of 0.3 nm [65].

The mLC model predictions [4] were based on collapse pressures obtained experimentally on solu-

tions having a mixture of tube chiralities. The collapse pressures were then obtained from the drop-vanishing of RBM intensity, procedure which we have followed here. We note the good correspondence between our observations of RBM vanishing and the mLC predictions. All previous Raman studies of carbon nanotube collapsing concerned samples having mixtures of tube chiralities, which prevented establishing a correspondence between the pressure evolution of the G-band – for which all tubes are resonant – with the diameter-discriminated signal of the RBMs. In the present work, the G-band evolution can be directly related to the (6,5) tubes having a diameter of 0.75 nm. The onset and end of the collapse, as predicted by the mLC model, correspond to two accidents observed in the evolution of the empty tubes G-band. Unfortunately, this very same pressure domain lies in the solidification region of the 4:1 methanol:ethanol PTM, which complicates the interpretation.

We have gathered in Fig. 5(a) our collapse pressure values with experimental results in literature for different empty and filled SWCNT. The graph shows the measured collapse pressure as a function of the tube diameter. The continuous line correspond to the modified Lévy-Carrier collapse pressure of empty SWCNT [4] and the shading around the line to its uncertainty. In addition to water or iodine, other simple or mixed fillers were considered. The different molecular filled nanotubes correspond to arc-discharge SWCNT which are mixed chirality systems but having low diameter dispersion in which the collapse pressure values were obtained with different spectroscopic criteria which as given in Table S2 of the S.I. [7, 14, 29, 32, 64]. In Table S2 of the S.I we also give the corrected collapsed pressures using the spectroscopic criterion for the collapse pressure for the G-band. Remarkably, some collapse pressure values for the same molecular filling which appeared as extremely incoherent in the different publications, become much intelligible now. This is for instance the case of argon filling for which collapse pressures >40 GPa [64] or 11 GPa [29], lie both now in a domain between 10 and 14 GPa.

Remarkably, all the molecule-filled SWCNT studied – *i.e* a total of 13 systems represented by solid symbols in the figure – show a higher collapse pressure than the corresponding empty tubes (open symbols). The experimental values of the empty tubes collapse pressure were obtained with our same RBM spectroscopic criterion [4]. We may define a stability factor $\Gamma = P_c^f / P_c^e$ characterizing the enhancement of the radial collapsing pressure by the filling of the tubes, where P_c^e and P_c^f are the empty and filled tube collapse pressures, respectively. We observe in Fig. 5(b) that Γ is larger for large diameter tubes. We note that there is a strong scattering of the collapse pressure in filled tubes, which may not only be explained by the nature of the filler but also by the filling rate which has been shown to have a strong influence on the collapse pressure value [11, 66] or the filling homogeneity [62]. Γ appears to be a complex function including dependencies on the tube diameter, the nature of the filler or the filling rate. In addition, as in any other high pressure experiment, the non-hydrostaticity of the pressure transmitting medium can also affect the collapse pressure and hence the

value of Γ. We also show in Fig. 5(b) the expected value of Γ for tubes filled with nanotubes obtained using the collapse pressure for MWCNT given in Ref. [4] but using as limiting value for the smallest possible supported nanotube, 0.3 nm [65]. We observe that molecular-filling offers a remarkably enhanced CNT radial stability as compared to tube-filling.

Let us note that both empty and iodine-filled SWCNT RBM peaks are partially retrieved after the pressure cycle (Fig. 2), with an empty tube signal intensity relative to the polyiodine components comparable to the one before pressure was applied. As the empty tubes are collapsed at 9 GPa and the maximum pressure reached is 51 GPa, it is unlikely that the initially empty tubes survive the pressure cycle unscathed [7, 28]. Instead, the iodine-filled tubes are most likely emptied of their iodine when collapsing, resulting in retrieving the empty tubes signal. This is corroborated by the blueshift of the high energy polyiodine feature upon pressure release, which indicates the occurrence of nonlinear polyiodine chains after the pressure cycle – which would be explained by the presence of free, non adsorbed iodine. Finally, our calculations show the formation of some I-C bonds associated with the pressure-induced collapsing of iodine filled (6,5) SWCNT. Although our experiments do not provide clear evidence of this, it can be a factor contributing to the opening of some tubes and the subsequent release of free iodine after a pressure cycle.

The evolution under pressure of the 1D iodine structure encapsulated in the CNT constitutes by itself an interesting subject. In fact, applying pressure was shown to affect the bonding structure of bulk halogens even at moderate pressures [67–69]. The iodine encapsulated in CNT with typical diameters of ~ 1.3 nm shows an evolution of the polyanion distribution with pressure favoring either iodine metallization or the formation of shorter polyanion groups [14]. In our experiments, we observe that the Raman peaks attributed to the polyanions are strongly upshifted at the collapse pressure of the iodine filled CNT. This is quite different from results on larger tubes where the iodine Raman peaks did not show discontinuities at the collapse pressure, but just a slight change of their pressure slope [14]. Our calculations did not allow to observe the initial formation of polyanions at ambient pressures. This has been observed in another work [70], but their *ab initio* computations were difficult to implement in the case of our high pressure study of chiral (6,5) tubes, as the unit cell is rather long and contains a large number of atoms.

We have only considered internal tube molecular filling in good correspondence with the HRTEM observations on I@(6,5) samples. Is there a possibility for some inter-tube intercalation which we should have not detected by HRTEM? Halogens inter-tube intercalation has been in fact observed in other works but shown to reduce the value of the collapse pressure with respect to empty tubes [71]. We can then safely exclude inter-tube iodine intercalation in our study. In the case of water filling, experiments show a lower pressure stabilization effect which could be interpreted as due to some partial inter-tube filling. Nevertheless, the excellent agreement of DFTB and experimental results on the weaker Γ values, coupled with the absence of

water inter-tube filling in our calculations, are also in favor of the absence of any significant inter-tube intercalation.

There remains a number of questions which have not been addressed in the present work, as for instance the effect of temperature on the stability of filled nanotubes. It has been shown that a higher temperature contributes to stabilizing the circular cross-section in large diameter SWCNT [72]. We may expect that the additional thermal agitation of encapsulated molecules could then further enhance the nanotube stability. Nevertheless, we may expect that the thermal contribution to the nanotube stability becomes negligible for low diameter tubes where the elastic energy is the dominant term.

Another aspect which was not addressed in the present work is a potential evolution of the bundle degree between pristine and filled nanotubes. In fact, we cannot exclude that the different manipulations leading to the nanotubes filling could quantitatively modify the bundling degree. As a matter of fact, modelling predicts a lower stability for bundles than for individualized nanotubes [5]. Nevertheless, such an effect being related to the surface tension of the outer bundle surface, it is only expected to have a significant effect for large diameter tubes only [5] and hence again, as for thermal effects, we do not expect a significant contribution for (6,5) tubes.

5. Conclusions

We performed *in situ* high pressure experimental studies on *single chirality* SWCNT using Raman spectroscopy combined with DFTB atomistic modelling. Our study shows an increasing radial stability of the (6,5) SWCNT once filled with a 1D-chain of molecules with respect to the pristine tubes. Moreover, iodine filling leads to an improved stability with respect to water filling. Our single chirality study allows to establishing a clear spectroscopic signature for the onset of the collapse pressure through the correlated drop of the RBM intensity and the G-band wavenumber softening. This criteria applied to the existing literature leads to more coherent and correlated results. Finally, we compared our results with the collapse pressure of empty and filled SWCNT of different diameters. This comparison shows that the radial collapsing of SWCNT is significantly enhanced with molecular filling having a superior effect to filling with other nanotubes (MWCNT). The obtained enhancement is strongly dependent on the filling species, but may also be affected by other aspects as hydrostaticity, filling ratio or homogeneity. These results show that molecular filling may be used as a superior method to improve the mechanical stability of carbon nanotubes either in device applications, cable production or in the elaboration of nanocomposites.

6. Acknowledgements

We acknowledge support from the iMUST LABEX program MUSCAT-2D. This work has been done thanks to the support of the high-pressure PLECE platform of the University of Lyon. CN thanks the financial support of China Scholarship Council (Scholarship number: #201306140037). SDSS acknowledges the support from the "Science Without Borders" program of the

CNPq/Brazil (Grant 248850/2013-0)

References

[1] Y. W. Sun, D. G. Papageorgiou, C. J. Humphreys, D. J. Dunstan, P. Puech, J. E. Proctor, C. Bousige, D. Machon, A. San Miguel, Mechanical properties of graphene, Appl. Phys. Rev. 8 (2021) 021310. doi:10.1063/5.0040578.

[2] J. A. Elliott, J. K. W. Sandler, A. H. Windle, R. J. Young, M. S. P. Shaffer, Collapse of Single-Wall Carbon Nanotubes is Diameter Dependent, Phys. Rev. Lett. 92 (9) (2004) 095501. doi:10.1103/PhysRevLett.92.095501.

[3] T. F. Cerqueira, S. Botti, A. San-Miguel, M. A. Marques, Density-functional tight-binding study of the collapse of carbon nanotubes under hydrostatic pressure, Carbon 69 (0) (2014) 355–360. doi:10.1016/j.carbon.2013.12.036.

[4] A. C. Torres-Dias, T. F. Cerqueira, W. Cui, M. A. Marques, S. Botti, D. Machon, M. A. Hartmann, Y. Sun, D. J. Dunstan, A. San-Miguel, From mesoscale to nanoscale mechanics in single-wall carbon nanotubes, Carbon 123 (2017) 145–150. doi:10.1016/j.carbon.2017.07.036.

[5] Y. Magnin, F. Rondepierre, W. Cui, D. J. Dunstan, A. San-Miguel, Collapse phase diagram of carbon nanotubes with arbitrary number of walls. Collapse modes and macroscopic analog, Carbon 178 (2021) 552–562. doi:10.1016/j.carbon.2021.03.031.

[6] M. Dresselhaus, G. Dresselhaus, R. Saito, Physics of carbon nanotubes, Carbon 33 (7) (1995) 883–891. doi:10.1016/0008-6223(95)00017-8.

[7] A. C. Torres-Dias, S. Cambré, W. Wenseleers, D. Machon, A. San-Miguel, Chirality-dependent mechanical response of empty and water-filled single-wall carbon nanotubes at high pressure, Carbon 95 (2015) 442–451. doi:10.1016/j.carbon.2015.08.032.

[8] M. He, J. Dong, K. Zhang, F. Ding, H. Jiang, A. Loiseau, J. Lehtonen, E. I. Kauppinen, Precise determination of the threshold diameter for a single-walled carbon nanotube to collapse, ACS Nano 8 (9) (2014) 9657–9663. doi:10.1021/nn5042812.

[9] Y. R. Poudel, W. Li, Synthesis, properties, and applications of carbon nanotubes filled with foreign materials: A review, Materials Today Physics 7 (2018) 7–34. doi:10.1016/j.mtphys.2018.10.002.

[10] R. S. Alencar, A. L. Aguiar, R. S. Ferreira, R. Chambard, B. Jousselme, J. L. Bantignies, C. Weigel, S. Clément, R. Aznar, D. Machon, A. G. Souza Filho, A. San-Miguel, L. Alvarez, Raman resonance tuning of quaterthiophene in filled carbon nanotubes at high pressures, Carbon 173 (2021) 163–173. doi:10.1016/j.carbon.2020.10.083.

[11] W. Cui, T. F. T. Cerqueira, S. Botti, M. A. L. Marques, A. San-Miguel, Nanostructured water and carbon dioxide inside collapsing carbon nanotubes at high pressure, Phys Chem Chem Phys 18 (29) (2016) 19926–19932. doi:10.1039/c6cp03263j.

[12] W. Q. Neves, R. S. Alencar, R. S. Ferreira, A. C. Torres-Dias, N. F. Andrade, A. San-Miguel, Y. A. Kim, M. Endo, D. W. Kim, H. Muramatsu, A. L. Aguiar, A. G. Souza Filho, Effects of pressure on the structural and electronic properties of linear carbon chains encapsulated in double wall carbon nanotubes, Carbon 133 (2018) 446–456. doi:10.1016/j.carbon.2018.01.084.

[13] C.-C. Ling, Q.-Z. Xue, L.-Y. Chu, N.-N. Jing, X.-Y. Zhou, Radial collapse of carbon nanotubes without and with stone–wales defects under hydrostatic pressure, RSC Adv. 2 (2012) 12182–12189. doi:10.1039/C2RA21581K.

[14] L. Alvarez, J.-L. Bantignies, R. Le Parc, R. Aznar, J.-L. Sauvajol, A. Merlen, D. Machon, A. San Miguel, High-pressure behavior of polyiodides confined into single-walled carbon nanotubes: A Raman study, Phys Rev B 82 (20) (2010) 205403. doi:10.1103/physrevb.82.205403.

[15] F. Balima, S. Le Floch, C. Adessi, T. F. Cerqueira, N. Blanchard, R. Arenal, A. Brûlet, M. A. Marques, S. Botti, A. San-Miguel, Radial collapse of carbon nanotubes for conductivity optimized polymer composites, Carbon 106 (2016) 64–73. doi:https://doi.org/10.1016/j.carbon.2016.05.004.

[16] D. Machon, V. Pischedda, S. Le Floch, A. San-Miguel, Perspective: High pressure transformations in nanomaterials and opportunities in material design, Jour-

nal of Applied Physics 124 (16) (2018) 160902. doi:10.1063/1.5045563.

[17] A. Kumar, K. Sharma, A. R. Dixit, A review on the mechanical properties of polymer composites reinforced by carbon nanotubes and graphene, Carbon Lett. 31 (2) (2021) 149–165. doi:10.1007/s42823-020-00161-x.

[18] C. Caillier, A. Ayari, V. Gouttenoire, J.-M. Benoit, V. Jourdain, M. Picher, M. Paillet, S. L. Floch, S. T. Purcell, J.-L. Sauvajol, A. S. Miguel, An Individual Carbon Nanotube Transistor Tuned by High Pressure, Adv. Funct. Mater. 20 (19) (2010) 3330–3335. doi:10.1002/adfm.201000398.

[19] W. Obitayo, T. Liu, A Review: Carbon Nanotube-Based Piezoresistive Strain Sensors, J. Sens. 2012 (2012) e652438. doi:10.1155/2012/652438.

[20] S. Rols, I. N. Goncharenko, R. Almairac, J. L. Sauvajol, I. Mirebeau, Polygonization of single-wall carbon nanotube bundles under high pressure, Phys. Rev. B 64 (2001) 153401. doi:10.1103/PhysRevB.64.153401.

[21] S. Karmakar, S. M. Sharma, A. Sood, Studies on high pressure behavior of carbon nanotubes: X-ray diffraction measurements using synchrotron radiation, Nuclear Instruments and Methods in Physics Research Section B: Beam Interactions with Materials and Atoms 238 (1) (2005) 281–284, synchrotron Radiation in Materials Science. doi:https://doi.org/10.1016/j.nimb.2005.06.064.

[22] R. S. Deacon, K.-C. Chuang, J. Doig, I. B. Mortimer, R. J. Nicholas, Photoluminescence study of aqueous-surfactant-wrapped single-walled carbon nanotubes under hydrostatic pressure, Phys. Rev. B 74 (2006) 201402. doi:10.1103/PhysRevB.74.201402.

[23] C. A. Kuntscher, A. Abouelsayed, K. Thirunavukkuarasu, F. Hennrich, Pressure-induced phenomena in single-walled carbon nanotubes: Structural phase transitions and the role of pressure transmitting medium, physica status solidi (b) 247 (11-12) (2010) 2789–2792. doi:https://doi.org/10.1002/pssb.201000150.

[24] B. Anis, F. Börrnert, M. H. Rümmeli, a. C. A. Kuntscher, Optical Microspectroscopy Study of the Mechanical Stability of Empty and Filled Carbon Nanotubes under Hydrostatic Pressure, J. Phys. Chem. C 118 (46) (2014) 27048–27062. doi:10.1021/jp506922s.

[25] M. Monteverde, M. Núñez Regueiro, Pressure control of conducting channels in single-wall carbon nanotube networks, Phys. Rev. Lett. 94 (2005) 235501. doi:10.1103/PhysRevLett.94.235501.

[26] A. L. Aguiar, E. B. Barros, R. B. Capaz, A. G. Souza Filho, P. T. C. Freire, J. M. Filho, D. Machon, C. Caillier, Y. A. Kim, H. Muramatsu, M. Endo, A. San-Miguel, Pressure-Induced Collapse in Double-Walled Carbon Nanotubes: Chemical and Mechanical Screening Effects, J. Phys. Chem. C 115 (13) (2011) 5378–5384. doi:10.1021/jp110675e.

[27] R. S. Alencar, A. L. Aguiar, A. R. Paschoal, P. T. C. Freire, Y. A. Kim, H. Muramatsu, M. Endo, H. Terrones, M. Terrones, A. San-Miguel, M. S. Dresselhaus, A. G. Souza Filho, Pressure-Induced Selectivity for Probing Inner Tubes in Double- and Triple-Walled Carbon Nanotubes: A Resonance Raman Study, J. Phys. Chem. C 118 (15) (2014) 8153–8158. doi:10.1021/jp4126045.

[28] S. Silva-Santos, R. Alencar, A. Aguiar, Y. Kim, H. Muramatsu, M. Endo, N. Blanchard, A. San-Miguel, A. Souza Filho, From high pressure radial collapse to graphene ribbon formation in triple-wall carbon nanotubes, Carbon 141 (2019) 568–579. doi:10.1016/j.carbon.2018.09.076.

[29] A. Merlen, P. Toulemonde, N. Bendiab, A. Aouizerat, J. L. Sauvajol, G. Montagnac, H. Cardon, P. Petit, A. S. Miguel, Raman spectroscopy of open-ended Single Wall Carbon Nanotubes under pressure: Effect of the pressure transmitting medium, Phys. Status Solidi B 243 (3) (2006) 690–699. doi:10.1002/pssb.200541364.

[30] J. E. Proctor, M. P. Halsall, A. Ghandour, D. J. Dunstan, High pressure raman spectroscopy of single-walled carbon nanotubes: Effect of chemical environment on individual nanotubes and the nanotube bundle, Journal of Physics and Chemistry of Solids 67 (12) (2006) 2468–2472. doi:https://doi.org/10.1016/j.jpcs.2006.06.024.

[31] D. Christofilos, J. Arvanitidis, K. S. Andrikopoulos, G. A. Kourouklis, S. Ves, T. Takenobu, Y. Iwasa, Comparative high pressure raman study of individual and bundled single-wall carbon nanotubes, physica status

solidi (b) 244 (1) (2007) 100–104. doi:https://doi.org/10.1002/pssb.200672568.

[32] C. Caillier, D. Machon, A. San-Miguel, R. Arenal, G. Montagnac, H. Cardon, M. Kalbac, M. Zukalova, L. Kavan, Probing high-pressure properties of single-wall carbon nanotubes through fullerene encapsulation, Phys Rev B 77 (12) (2008) 125418. doi:10.1103/PhysRevB.77.125418.

[33] A. J. Ghandour, D. J. Dunstan, A. Sapelkin, J. E. Proctor, M. P. Halsall, High-pressure raman response of single-walled carbon nanotubes: Effect of the excitation laser energy, Phys. Rev. B 78 (2008) 125420. doi:10.1103/PhysRevB.78.125420.

[34] M. Yao, Z. Wang, B. Liu, Y. Zou, S. Yu, W. Lin, Y. Hou, S. Pan, M. Jin, B. Zou, T. Cui, G. Zou, B. Sundqvist, Raman signature to identify the structural transition of single-wall carbon nanotubes under high pressure, Phys. Rev. B 78 (2008) 205411. doi:10.1103/PhysRevB.78.205411.

[35] A. Merlen, P. Toulemonde, S. Le Floch, G. Montagnac, T. Hammouda, O. Marty, A. San Miguel, High pressure-high temperature synthesis of diamond from single-wall pristine and iodine doped carbon nanotube bundles, Carbon 47 (7) (2009) 1643–1651. doi:10.1016/j.carbon.2009.02.014.

[36] A. J. Ghandour, I. F. Crowe, J. E. Proctor, Y. W. Sun, M. P. Halsall, I. Hernandez, A. Sapelkin, D. J. Dunstan, Pressure coefficients of raman modes of carbon nanotubes resolved by chirality: Environmental effect on graphene sheet, Phys. Rev. B 87 (2013) 085416. doi:10.1103/PhysRevB.87.085416.

[37] M. S. Dresselhaus, A. Jorio, M. Hofmann, G. Dresselhaus, R. Saito, Perspectives on carbon nanotubes and graphene raman spectroscopy, Nano Letters 10 (3) (2010) 751–758. doi:10.1021/nl904286r.

[38] L. Malard, M. Pimenta, G. Dresselhaus, M. Dresselhaus, Raman spectroscopy in graphene, Phys. Rep. 473 (2009) 51–87. doi:10.1016/j.physrep.2009.02.003.

[39] D. Machon, C. Bousige, R. Alencar, A. Torres-Dias, F. Balima, J. Nicolle, G. S. Pinhero, A. G. de Souza Filho, A. S. Miguel, Raman scattering studies of graphene under high pressure, J Raman Spectrosc 49 (2018) 121–129. doi:10.1002/jrs.5284.

[40] N. K. Subbaiyan, S. Cambré, A. N. G. Parra-Vasquez, E. H. Hároz, S. K. Doorn, J. G. Duque, Role of Surfactants and Salt in Aqueous Two-Phase Separation of Carbon Nanotubes toward Simple Chirality Isolation, ACS Nano 8 (2014) 1619–1628. doi:10.1021/nn405934y.

[41] N. K. Subbaiyan, A. N. G. Parra-Vasquez, S. Cambré, M. A. S. Cordoba, S. E. Yalcin, C. E. Hamilton, N. H. Mack, J. L. Blackburn, S. K. Doorn, J. G. Duque, Bench-top aqueous two-phase extraction of isolated individual single-walled carbon nanotubes, Nano Res. 8 (5) (2015) 1755–1769. doi:10.1007/s12274-014-0680-z.

[42] C. Bousige, S. Rols, E. Paineau, S. Rouzière, C. Mocuta, B. Verberck, J. P. Wright, H. Kataura, P. Launois, Progressive melting in confined one-dimensional C_{60} chains, Phys Rev B 86 (4) (2012) 045446. doi:10.1103/PhysRevB.86.045446.

[43] C. Bousige, S. Rols, J. Ollivier, H. Schober, P. Fouquet, G. G. Simeoni, V. Agafonov, V. Davydov, Y. Niimi, K. Suenaga, H. Kataura, P. Launois, From a one-dimensional crystal to a one-dimensional liquid: A comprehensive dynamical study of C_{60} peapods, Phys Rev B 87 (19) (2013) 195438. doi:10.1103/PhysRevB.87.195438.

[44] C. Nie, A.-M. Galibert, B. Soula, E. Flahaut, J. Sloan, M. Monthioux, A new insight on the mechanisms of filling closed carbon nanotubes with molten metal iodides, Carbon 110 (2016) 48–50. doi:10.1016/j.carbon.2016.09.001.

[45] S. Cambré, B. Schoeters, S. Luyckx, E. Goovaerts, W. Wenseleers, Experimental observation of single-file water filling of thin single-wall carbon nanotubes down to chiral index (5,3), Phys. Rev. Lett. 104 (2010) 207401. doi:10.1103/PhysRevLett.104.207401.

[46] Y. Piao, J. R. Simpson, J. K. Streit, G. Ao, M. Zheng, J. A. Fagan, A. R. Hight Walker, Intensity ratio of resonant raman modes for (n,m) enriched semiconducting carbon nanotubes, ACS Nano 10 (5) (2016) 5252–5259. arXiv:https://doi.org/10.1021/acsnano.6b01031, doi:10.1021/acsnano.6b01031.

[47] A. D. Chijioke, W. Nellis, A. Soldatov, I. F. Silvera, The ruby pressure standard to 150 GPa, J Appl Phys

98 (11) (2005) 114905. doi:10.1063/1.2135877.

[48] S. Klotz, J. Chervin, P. Munsch, G. Le Marchand, Hydrostatic limits of 11 pressure transmitting media, J Phys Appl Phys 42 (7) (2009) 075413. doi:10.1088/0022-3727/42/7/075413.

[49] R. Letoullec, J. P. Pinceaux, P. Loubeyre, The membrane diamond anvil cell: A new device for generating continuous pressure and temperature variations, High Press. Res. 1 (1) (1988) 77–90. doi:10.1080/08957958808202482.

[50] A. San-Miguel, Nanomaterials under high-pressure, Chem Soc Rev 35 (10) (2006) 876–889. doi:10.1039/b517779k.

[51] B. Aradi, B. Hourahine, T. Frauenheim, DFTB+, a Sparse Matrix-Based Implementation of the DFTB Method, J. Phys. Chem. A 111 (26) (2007) 5678–5684. doi:10.1021/jp070186p.

[52] B. Hourahine, B. Aradi, V. Blum, F. Bonafé, A. Buccheri, C. Camacho, C. Cevallos, M. Y. Deshaye, T. Dumitrică, A. Dominguez, S. Ehlert, M. Elstner, T. van der Heide, J. Hermann, S. Irle, J. J. Kranz, C. Köhler, T. Kowalczyk, T. Kubař, I. S. Lee, V. Lutsker, R. J. Maurer, S. K. Min, I. Mitchell, C. Negre, T. A. Niehaus, A. M. N. Niklasson, A. J. Page, A. Pecchia, G. Penazzi, M. P. Persson, J. Řezáč, C. G. Sánchez, M. Sternberg, M. Stöhr, F. Stuckenberg, A. Tkatchenko, V. W.-z. Yu, T. Frauenheim, DFTB+, a software package for efficient approximate density functional theory based atomistic simulations, J. Chem. Phys. 152 (12) (2020) 124101. doi:10.1063/1.5143190.

[53] R. S. Alencar, W. Cui, A. C. Torres-Dias, T. F. T. Cerqueira, S. Botti, M. A. L. Marques, O. P. Ferreira, C. Laurent, A. Weibel, D. Machon, D. J. Dunstan, A. G. Souza Filho, A. San-Miguel, Pressure-induced radial collapse in few-wall carbon nanotubes: A combined theoretical and experimental study, Carbon 125 (2017) 429–436. doi:10.1016/j.carbon.2017.09.044.

[54] J. Frenzel, A. F. Oliveira, H. A. Duarte, T. Heine, G. Seifert, Structural and Electronic Properties of Bulk Gibbsite and Gibbsite Surfaces, Z. Für Anorg. Allg. Chem. 631 (6-7) (2005) 1267–1271. doi:10.1002/zaac.200500051.

[55] T. Kubař, Z. Bodrog, M. Gaus, C. Köhler, B. Aradi, T. Frauenheim, M. Elstner, Parametrization of the SCC-DFTB Method for Halogens, J. Chem. Theory Comput. 9 (7) (2013) 2939–2949. doi:10.1021/ct4001922.

[56] M. Elstner, D. Porezag, G. Jungnickel, J. Elsner, M. Haugk, T. Frauenheim, S. Suhai, G. Seifert, Self-consistent-charge density-functional tight-binding method for simulations of complex materials properties, Phys. Rev. B 58 (11) (1998) 7260–7268. doi:10.1103/PhysRevB.58.7260.

[57] L. Grigorian, K. A. Williams, S. Fang, G. U. Sumanasekera, A. L. Loper, E. C. Dickey, S. J. Pennycook, P. C. Eklund, Reversible Intercalation of Charged Iodine Chains into Carbon Nanotube Ropes, Phys. Rev. Lett. 80 (25) (1998) 5560–5563. doi:10.1103/PhysRevLett.80.5560.

[58] U. D. Venkateswaran, E. A. Brandsen, M. E. Katakowski, A. Harutyunyan, G. Chen, A. L. Loper, P. C. Eklund, Pressure dependence of the Raman modes in iodine-doped single-walled carbon nanotube bundles, Phys Rev B 65 (5) (2002) 054102. doi:10.1103/physrevb.65.054102.

[59] W. Zhou, S. Xie, L. Sun, D. Tang, Y. Li, Z. Liu, L. Ci, X. Zou, G. Wang, P. Tan, X. Dong, B. Xu, B. Zhao, Raman scattering and thermogravimetric analysis of iodine-doped multiwall carbon nanotubes, Appl. Phys. Lett. 80 (14) (2002) 2553–2555. doi:10.1063/1.1468269.

[60] P. Deplano, J. R. Ferraro, M. L. Mercuri, E. F. Trogu, Structural and Raman spectroscopic studies as complementary tools in elucidating the nature of the bonding in polyiodides and in donor-I2 adducts, Coordination Chemistry Reviews 188 (1) (1999) 71–95. doi:10.1016/S0010-8545(98)00238-0.

[61] M. Hanfland, H. Beister, K. Syassen, Graphite under pressure: Equation of state and first-order Raman modes, Phys Rev B 39 (17) (1989) 12598. doi:10.1103/PhysRevB.39.12598.

[62] A. L. Aguiar, R. B. Capaz, A. G. Souza Filho, A. San-Miguel, Structural and phonon properties of bundled single- and double-wall carbon nanotubes under pressure, The Journal of Physical Chemistry C 116 (42) (2012) 22637–22645. doi:10.1021/jp3093176.

[63] P. A. Djondjorov, V. M. Vassilev, I. M. Mladenov, Analytic description and explicit parametrisation of the equilibrium shapes of elastic rings and tubes under uniform hydrostatic pressure, International Journal of Mechanical Sciences 53 (5) (2011) 355–364. doi:10.1016/j.ijmecsci.2011.02.005.

[64] A. Merlen, N. Bendiab, P. Toulemonde, A. Aouizerat, A. San Miguel, J. L. Sauvajol, G. Montagnac, H. Cardon, P. Petit, Resonant raman spectroscopy of single-wall carbon nanotubes under pressure, Phys. Rev. B 72 (2005) 035409. doi:10.1103/PhysRevB.72.035409.

[65] X. Zhao, Y. Liu, S. Inoue, T. Suzuki, R. O. Jones, Y. Ando, Smallest carbon nanotube is 3å in diameter, Phys. Rev. Lett. 92 (2004) 125502. doi:10.1103/PhysRevLett.92.125502.

[66] Y. Zheng, H. He, H. Ye, Radial stability and configuration transition of carbon nanotubes regulated by enclosed cores, AIP Advances 5 (5) (2015) 057155. doi:10.1063/1.4921889.

[67] A. San Miguel, H. Libotte, J. Gaspard, M. Gauthier, J. Itié, A. Polian, Bromine metallization studied by X-ray absorption spectroscopy, Eur. Phys. J. B 17 (2) (2000) 227–233. doi:10.1007/s100510070136.

[68] A. San-Miguel, H. Libotte, M. Gauthier, G. Aquilanti, S. Pascarelli, J.-P. Gaspard, New Phase Transition of Solid Bromine under High Pressure, Phys. Rev. Lett. 99 (1) (2007) 015501. doi:10.1103/PhysRevLett.99.015501.

[69] J. Shi, E. Fonda, S. Botti, M. A. L. Marques, T. Shinmei, T. Irifune, A.-M. Flank, P. Lagarde, A. Polian, J.-P. Itié, A. San-Miguel, Halogen molecular modifications at high pressure: The case of iodine, Phys. Chem. Chem. Phys. 23 (5) (2021) 3321–3326. doi:10.1039/D0CP05942K.

[70] H.-P. Komsa, R. Senga, K. Suenaga, A. V. Krasheninnikov, Structural Distortions and Charge Density Waves in Iodine Chains Encapsulated inside Carbon Nanotubes, Nano Lett. 17 (6) (2017) 3694–3700. doi:10.1021/acs.nanolett.7b00969.

[71] A. L. Aguiar, E. B. Barros, V. P. Sousa Filho, H. Terrones, V. Meunier, D. Machon, Y. A. Kim, H. Muramatsu, M. Endo, F. Baudelet, A. San-Miguel, A. G. Souza Filho, Pressure tuning of bromine ionic states in double-walled carbon nanotubes, The Journal of Physical Chemistry C 121 (19) (2017) 10609–10619. arXiv:https://doi.org/10.1021/acs.jpcc.7b03187, doi:10.1021/acs.jpcc.7b03187.

[72] T. Chang, Z. Guo, Temperature-induced reversible dominoes in carbon nanotubes, Nano Letters 10 (9) (2010) 3490–3493, pMID: 20681525. arXiv:https://doi.org/10.1021/nl101623c, doi:10.1021/nl101623c.